



Published in final edited form as:

Nat Commun. ; 1: 90. doi:10.1038/ncomms1085.

A subunit-selective potentiator of NR2C- and NR2D-containing NMDA receptors

Praseeda Mullasseril¹, Kasper B. Hansen¹, Katie M. Vance¹, Kevin K. Ogden¹, Hongjie Yuan¹, Natalie L. Kurtkaya¹, Rose Santangelo², Anna G. Orr¹, Phuong Le¹, Kimberly M. Vellano¹, Dennis C. Liotta², and Stephen F. Traynelis^{1,*}

¹Department of Pharmacology, Emory University School of Medicine, Atlanta GA 30322

²Department of Chemistry, Emory University, Atlanta GA 30322

Abstract

NMDA receptors are tetrameric complexes of NR1 and NR2A-D subunits that mediate excitatory synaptic transmission and play a role in neurological disorders. We have identified a novel subunit-selective potentiator of NMDA receptors containing the NR2C or NR2D subunit, which could allow selective modification of circuit function in regions expressing NR2C/D subunits. The substituted tetrahydroisoquinoline CIQ enhances receptor responses two-fold with an EC₅₀ of 3 μM by increasing channel opening frequency without altering mean open time or EC₅₀ values for glutamate or glycine. The actions of CIQ depend on a single residue in the M1 region (NR2D Thr592) and the linker between the amino terminal domain and agonist binding domain. CIQ potentiates native NR2D-containing NMDA receptor currents from subthalamic neurons. Our identification of a subunit-selective NMDA receptor modulator reveals a new class of pharmacological tools with which to probe the role of NR2C- and NR2D-containing NMDA receptors in brain function and disease.

The involvement of NMDA receptors in neurological diseases including Alzheimer's disease, Parkinson's disease, depression, schizophrenia, epilepsy, and injury related to ischemia, hypoxia, or trauma¹⁻⁷ raises the possibility that compounds that potentiate or inhibit NMDA receptor function could have therapeutic benefit⁶⁻¹⁰. Compounds that selectively act at one NR2 subunit might modify neuronal function for therapeutic gain only in brain regions in which that subunit is expressed, minimizing side effects due to modulation of other NMDA receptors elsewhere. However, despite decades of work, there is only a single NR2 subunit, NR2B, for which there exist highly (> 500-fold) selective pharmacological tools¹¹⁻¹³.

The NR2 subunits show spatially distinct expression patterns throughout the CNS. For example, NR2A and NR2B are primarily expressed in rat cortex and hippocampus, whereas the NR2C subunit is highly expressed in cerebellar granule cells, retrosplenial cortex,

*Corresponding Author: Dr. Stephen Traynelis, Dept Pharmacology, Emory University School of Medicine, Rollins Research Center, 1510 Clifton Road, Atlanta, GA 30322-3090, Tel 404 727 0357, Fax 404 727 0365, strayne@emory.edu .

Author Contributions

PM, KBH, KMV, KKO, HY, NLK, AGO, PL, KMV, SFT all participated in identification of the initial class of tetrahydroisoquinoline potentiators, as well as recording and analysis of the data. RS, DCL, SFT participated in determination of the structure activity relationship leading to identification of CIQ. All authors participated in writing the manuscript.

Supplementary Information

Supplementary methods and figures accompany the paper.

Competing interests

Some of the authors (DCL, RS, SFT) are co-inventors on Emory University-owned intellectual property for which a patent application has been filed (Subunit-selective NMDA receptor potentiators for the treatment of neurological conditions, PCT/US2010/22439).

thalamus, pontine and vestibular nuclei, and oligodendrocytes¹⁴⁻¹⁹. The NR2D subunit is expressed in deep cerebellar nuclei, subthalamic neurons, striatal neurons, and substantia nigra dopaminergic neurons^{14-16,20-25}. Interestingly, both NR2C and NR2D mRNA are expressed in hippocampal and cortical interneurons^{15,21-22,26-28}. The regional and cell-specific expression of the NR2 subunits in the brain coupled with the lack of subunit-selective pharmacological tools motivated us to search for subunit-selective allosteric modulators, which could be useful tools for evaluating the functional role of individual NMDA receptor subunits in normal brain function and in animal models of neurological diseases. We thus evaluated the activity of 100,000 compounds against NR1/NR2C or NR1/NR2D receptors, and identified a class of novel tetrahydroisoquinolines that selectively enhance the responses of NR2C- and NR2D-containing NMDA receptors.

Results

Subunit selectivity and mechanism of CIQ

Figure 1 shows the structure of (3-chlorophenyl)(6,7-dimethoxy-1-((4-methoxyphenoxy)methyl)-3,4-dihydroisoquinolin-2(1H)-yl)methanone (CIQ), a chiral compound that emerged from medicinal chemistry efforts to optimize the structure-activity relationship of a single tetrahydroisoquinoline initially identified during screening (See Methods and Supplementary Fig. S1). In the presence of both glutamate and glycine, CIQ potentiated the response of rat recombinant NR2C- or NR2D-containing NMDA receptors expressed in *Xenopus laevis* oocytes in a concentration-dependent fashion (Fig. 1a). Potentiation was reversible and repeatable. The EC₅₀ values for potentiation of NR2C- and NR2D-containing receptors were 2.7 and 2.8 μ M, respectively (maximal potentiation $197 \pm 20\%$ and $211 \pm 7\%$; n = 21, 18; Fig. 1b, Supplementary Table S1). Similar EC₅₀ values were found with different NR1 splice variants as well as with human NMDA receptors (Supplementary Table S2). In contrast to its effects on NR1/NR2C and NR1/NR2D receptors, CIQ (10 μ M) did not alter recombinant NR1/NR2A, NR1/NR2B, AMPA, or kainate receptor responses (Fig. 1).

To test whether CIQ could potentiate triheteromeric NMDA receptors containing one NR2C or NR2D subunit, we co-injected oocytes with NR1, NR2C or NR2D, and the magnesium-insensitive, low glutamate potency mutant NR2A(N614K, T690I) (hereafter denoted NR2A*)²⁹. Oocytes co-injected with NR2A* showed reduced Mg²⁺ sensitivity (Supplementary Fig. S2a). Moreover, the residual current recorded in the presence of 1 mM Mg²⁺ at a holding potential of -80 mV increased with increasing glutamate concentrations only for receptors in oocytes co-injected with NR1, NR2A*, NR2C or NR1, NR2A*, NR2D cRNAs (Supplementary Fig S2b). This suggests that higher glutamate concentrations can activate magnesium-insensitive NR2A*-containing receptors that could be either diheteromeric NR1/NR2A* or triheteromeric receptors containing one NR2A* subunit and one NR2C or NR2D. NR1/NR2C and NR1/NR2D receptors are saturated at all concentrations of glutamate tested (0.1-10 mM), and thus their contribution to the response does not change with increasing concentrations of glutamate.

CIQ significantly potentiated the current response recorded in the presence of Mg²⁺ from oocytes co-injected with NR1, NR2A*, NR2C or NR1, NR2A*, NR2D cRNA (Fig 1c), but to a lesser extent than NR1/NR2C and NR1/NR2D receptors recorded under identical conditions (Supplementary Fig. S3). Because Mg²⁺ did not completely inhibit NR1/NR2C or NR1/NR2D receptors (Supplementary Fig. S2a), the intermediate level of CIQ potentiation could be explained if no triheteromeric receptors formed and CIQ simply potentiated the residual NR1/NR2C or NR1/NR2D current (NR1/NR2A* receptors are not potentiated by CIQ, Supplementary Fig. S3). However, the level of CIQ potentiation observed in oocytes injected with NR1, NR2A*, NR2C or NR1, NR2A*, NR2C cRNA was

significantly greater ($p < 0.05$, Student's t-test; Supplementary Fig. S3) than the level of potentiation predicted if no triheteromeric receptors were present (see Methods), suggesting triheteromeric NR1/NR2A*/NR2C and NR1/NR2A*/NR2D receptors were present and were potentiated by CIQ. CIQ potentiation of triheteromeric receptors (Fig. 1c) implies that a single NR2C or NR2D subunit was sufficient to confer sensitivity to CIQ. CIQ had no effect on responses of NR1/NR2A*/NR2B receptors (Fig. 1c), and no effect on the properties of oocytes injected with cRNA for NR1, NR2A, or NR2B alone ($n = 5$).

CIQ did not potentiate recombinant NR1/NR2A ($n = 6$) and NR1/NR2B receptors ($n = 6$) expressed in oocytes and activated by the partial agonist NMDA (100 μM) plus glycine (30 μM). However, CIQ potentiated recombinant NR1/NR2C ($n = 6$) and NR1/NR2D receptors ($n = 5$) activated by 100 μM NMDA and 30 μM glycine ($233 \pm 13\%$, $205 \pm 5\%$) to the same extent as responses activated by glutamate ($p = 0.75$, 0.70 , unpaired t-test) with similar EC_{50} values (2.7 and 3.3 μM). Thus, the actions of CIQ do not depend on the agonist used to activate the receptor.

At peak potentiation, CIQ caused virtually no shift in the EC_{50} values for activation of NR1/NR2C or NR1/NR2D receptors by glutamate or glycine (Table 1). Importantly, CIQ alone had no effect on oocytes expressing NR1/NR2C ($n = 4$) or NR1/NR2D receptors ($n = 4$) or on uninjected oocytes ($n = 4$). CIQ also did not activate the receptor in the presence of only glycine ($n = 4$) or glutamate ($n = 4$), suggesting it does not act as an agonist. CIQ potentiated responses in the presence of extracellular Mg^{2+} without significantly altering the IC_{50} values for Mg^{2+} inhibition (Supplementary Table S1). Moreover, CIQ potentiation was not altered at acidic pH values, suggesting CIQ did not relieve tonic proton inhibition (Supplementary Table S1), as proposed for spermine potentiation of NR2B-containing receptors³⁰. The potentiating actions of CIQ appeared voltage-independent, with similar degrees of potentiation for both inward and outward currents (Supplementary Table S3). These data suggest CIQ binding is not allosterically coupled to agonist binding and does not exert its effects through alteration of permeation properties.

CIQ also potentiated current responses of NR2C- and NR2D-containing NMDA receptors expressed in HEK 293 cells at room temperature (23°C) and at 33°C (Fig. 2). Maximal potentiation was 180% for both NR1/NR2C and NR1/NR2D with EC_{50} values of 1.7 and 4.1 μM , respectively. The time course for the onset of potentiating effects of CIQ was exponential and required several seconds to reach steady-state (Fig. 2c). The potentiation by CIQ was rapidly reversible with a time course of de-potentiation that could be fitted by a single exponential component (NR1/NR2C tau 4.0 ± 0.7 s and NR1/NR2D tau 6.5 ± 0.7 s; $n = 3,6$). The de-potentiation time constant was independent of CIQ concentration (Fig. 2d). The 10-90% rise time of receptor response was rapid in the absence of CIQ (NR2C 6 ± 1 ms; NR2D 13 ± 1 ms) and following pre-application of CIQ (NR2C 9 ± 1 ms; NR2D 15 ± 2 ms), suggesting that CIQ does not require channel opening prior to binding. CIQ (10 μM) had minimal effects on the NMDA receptor deactivation time course (Table 2).

Single channel analysis of CIQ

To determine the mechanism by which CIQ enhanced the NMDA receptor response, the actions of CIQ on NMDA receptor single channel properties were examined. Application of 1 mM glutamate and 50 μM glycine to excised outside-out patches containing rat recombinant NR1/NR2D receptors produced unitary currents with properties similar to those previously described^{31,32}. Unitary currents showed two sublevels with chord conductance values of 33 and 56 pS in 0.5 mM extracellular Ca^{2+} . Co-application of 10 μM CIQ increased the open probability to $190 \pm 25\%$ of control ($n = 11$) in a reversible manner (Fig. 2e, Table 3). The effect of CIQ on open probability is due solely to an effect on mean shut time (Fig 2f), as CIQ decreased mean shut time to $75 \pm 8\%$ of control ($n = 11$). The mean

open time was unchanged by CIQ, as were individual fitted exponential components describing the open duration histogram (Fig. 2f, Table 3). CIQ had minimal effects on chord conductance and no detectable effect on the reversal potential. CIQ had no significant effect on the relative frequency of the lower conductance level and did not alter relative frequency of direct 33-56 pS or 56-33 pS sublevel transitions. These data suggest that CIQ binds to a site on the NMDA receptor that influences channel opening, without altering the stability of the open state or the nature of the permeation pathway. We interpret these data to suggest that CIQ likely acts to facilitate pre-gating steps that follow agonist binding and either precede or are involved in pore dilation.

Molecular determinants of CIQ

To identify the molecular determinants of CIQ activity, we measured responses of NMDA receptors containing NR2A-NR2D chimeric subunits (Fig. 3; see Supplementary Fig. S4 and Supplementary Table S4 for chimeric junctions). Taking advantage of the fact that CIQ potentiates NR1/NR2D receptors but not NR1/NR2A receptors, we first evaluated the portions of NR2D that when inserted into NR2A transferred CIQ-sensitivity. Evaluation of these chimeric receptors for a gain of function suggested that the molecular determinants of CIQ selectivity for NR2D over NR2A reside in the L-S1-M1 region (Fig. 3a,b). Further assessment of chimeric receptors containing progressively smaller portions of the NR2D subunit narrowed down the regions of interest to the linker (L) between the ATD and ligand binding domain plus five residues (590-594) in the M1 transmembrane helix of NR2D. The chimera NR2A-(2D L+M1e) containing only these two regions from NR2D was potentiated by 10 μ M CIQ (Fig. 3b). CIQ did not show any activity when the ATD-S1 linker (L) of NR2D alone was transferred to NR2A ($n = 16$), or when residues 590-594 in NR2D alone were transferred to NR2A ($n = 4$) (Supplementary Table S4). The open probability of NR1/NR2D (0.01) is lower than that of NR1/NR2A (0.5)³³, raising the possibility that CIQ facilitation of channel opening might require a low open probability. Consistent with this idea, the ATD-S1 linker (L) between the ATD and ligand binding domain of NR2D has previously been shown to reduce open probability when introduced into NR2A³³.

To identify the elements required for CIQ potentiation of NR2D, we evaluated a series of NR2D mutations for loss of function. Insertion of the NR2A ATD-S1 linker (L) into NR2D did not significantly alter CIQ potentiation (2D-(2A L); Fig. 4). CIQ potentiation of chimeric receptors in which both the NR2A ATD and ATD-S1 linker (2D-(2A ATD+L)) are placed into NR2D is attenuated (Fig. 4b). This result is consistent with the idea that some elements of the ATD beyond the linker enhance the actions of CIQ on NR2D. Site-directed mutagenesis within the M1 region of NR2D identified a single residue (Thr592) that is conserved in NR2C/D but different in NR2A/B as an important determinant of activity (Fig. 4b). In contrast to results with NR2D-(NR2A L) chimeric receptors, mutagenesis of this residue to the corresponding residue in NR2A (NR2D T592I) completely abolished the potentiating actions of CIQ (Fig. 4b). CIQ (10 μ M) significantly potentiated NR2A-containing receptors with the corresponding reverse mutation NR2A(I567T) and the linker (L) between NR2D ATD and S1 ($135 \pm 5\%$, $n = 12$). However, this point mutation in NR2A (I567T) along with the NR2D ATD-S1 linker was not sufficient to transfer the full CIQ potentiation observed at NR1/NR2D to NR1/NR2A (see Supplementary Table S4). These data show consistent gain of function and loss of function effects relating to residue Thr592 in the NR2D M1 region (Fig 3c). These data also identify the ATD and linker between ATD and S1, which has divergent sequences across all four NR2 subunits, as an important structural determinant of CIQ actions in NR2D (Fig 3c).

The actions of CIQ on native NMDA receptors

The NR2D subunit has been suggested to be the predominant NMDA receptor NR2 subunit expressed in neurons of the subthalamic nuclei²⁰. We therefore evaluated the ability of CIQ to potentiate native NMDA receptor responses in subthalamic neurons using whole cell voltage-clamp recordings of current responses to pressure application of NMDA and glycine in the absence of synaptic transmission. This approach provides tight control over the amount of agonist released, which activates both synaptic and extra-synaptic receptors (Fig. 5a). NMDA receptor responses were produced by pressure-release of agonist at 1 minute intervals in neurons held at -60 mV and bathed in ACSF containing 0.2 mM Mg^{2+} , 0.5 μ M TTX, 5 μ M nimodipine, and 10 μ M bicuculline. NMDA receptor responses were evaluated before, during, and after bath application of CIQ (20 μ M). CIQ potentiated NMDA-activated responses in 6 out of 6 subthalamic neurons by an average of $230 \pm 29\%$ ($n = 6$; Fig. 5b *white bars*, c). Potentiation by CIQ was reversible; responses after wash were not significantly different than control responses ($102 \pm 11\%$; $n = 6$; Fig. 5b,c). Application of vehicle alone had no significant effect on response amplitude to pressure-applied NMDA plus glycine ($106 \pm 9\%$, $n = 5$; $p = 0.25$). NMDA-activated responses could be largely inhibited by bath application of 200 - 400 μ M of the competitive NMDA receptor antagonist D,L-APV. CIQ did not potentiate NMDA-activated responses of CA1 hippocampal pyramidal neurons ($n = 5$; Fig. 5b *gray bars*, d), which have been shown to predominantly express NR2A and NR2B NMDA receptor subunits¹⁵, demonstrating that potentiation by CIQ is selective for native NR2C/D-containing NMDA receptors.

Discussion

The physiological, pharmacological, and biophysical properties of NMDA receptors are governed by the NR2 subunit¹. Despite the important role that NMDA receptors play in CNS function and neurological disorders, there remains a surprising lack of molecules that act on NMDA receptors with sufficient subunit-selectivity to allow evaluation of the role of NR2 subunits in normal function and disease. We report here the first drug-like NMDA receptor positive allosteric modulator (CIQ) that potentiates NR2C- and NR2D-containing NMDA receptor responses with strong subunit selectivity. Although the data do not unequivocally identify a binding site for CIQ, molecular studies reveal structural determinants of subunit selectivity, and support the idea that CIQ binds to a new modulatory site that is either near the NR2 M1 region or NR2 ATD and associated linker. Mechanistic studies suggest that CIQ binding reduces the activation energy for key conformational changes that lead to channel opening, without altering the stability of the open state. Studies of native receptors in the absence of synaptic transmission show that CIQ can potentiate NMDA receptor responses of subthalamic neurons to exogenously applied NMDA. Thus, CIQ represents a new class of subunit-selective NMDA receptor modulators with which to probe the role of NR2C- and NR2D-containing NMDA receptors in brain function and disease.

Methods

Two-electrode voltage-clamp recordings from *Xenopus laevis*

All procedures involving the use of animals were reviewed and approved by the Emory University IACUC. Oocytes from *Xenopus laevis* were isolated, injected with cRNA synthesized *in vitro*, and recorded under voltage-clamp as previously described³⁵. The recording solution contained (in mM) 90 NaCl, 3 KCl, 10 HEPES, 0.01 EDTA, 0.5 BaCl₂ (23° C); pH was adjusted to 7.4 with NaOH. Glutamate-evoked membrane currents (50 - 100 μ M) were recorded at -40 mV in the presence of 30 - 100 μ M glycine 24 - 72 hours after injection unless otherwise indicated.

Triheteromeric NMDA receptors comprised of NR1 and two different NR2 subunits were studied using the method of Hatton and Paoletti²⁹. Briefly, NR2B, NR2C, or NR2D cRNA were co-injected with cRNA encoding NR2A(N614K,T690I) (referred to as NR2A*) and NR1 at a ratio of 1:3:2 (20 ng total). Responses to glutamate (10 mM) and glycine (100 μM) were recorded at -80 mV 24-72 h post-injection. NR1/NR2A* receptors were insensitive to block by Mg²⁺ and had reduced glutamate potency. Thus, NR2A* should allow isolation of triheteromeric receptors when co-expressed with NR1 and NR2B, NR2C, or NR2D by recording in the presence of 1 mM Mg²⁺ and 10 mM glutamate²⁹. We estimated the maximum possible level of potentiation due solely to NR1/NR2C receptors in the residual response. If one assumes that no triheteromeric receptors were present in oocytes injected with NR1, NR2A*, NR2C cRNA, then the relative current in Mg²⁺ would be due solely to NR1/NR2C and NR1/NR2A* receptors, with the relative contribution determined by

$$\left(I_{Mg}/I_{Control}\right)_{2A^*/2C} = \alpha \left(I_{Mg}/I_{Control}\right)_{2C} + \beta \left(I_{Mg}/I_{Control}\right)_{2A^*} \text{ and } \alpha + \beta = 1$$

where α is the fraction of the current from NR1/NR2C receptors, β is the fraction of current from NR1/NR2A* receptors, and $(I_{Mg}/I_{Control})$ is the residual current response in the presence of 1 mM Mg²⁺ at -80 mV (Supplementary Fig. S2a). Assuming no triheteromeric receptors were formed, we can calculate $\alpha = 0.813$ and $\beta = 0.187$ from this equation for NR2C using the data shown in Supplementary Figure S2a. Because CIQ has no detectable effect on NR1/NR2A* receptors (Supplementary Fig. S3a), we can calculate the maximum possible CIQ potentiation due solely to residual NR1/NR2C according to the equation

$$\text{Maximum potentiation (\%)} = 100 \left(\alpha \left(I_{CIQ}/I_{Control} \right)_{2C} \left(I_{Mg}/I_{Control} \right)_{2C} + \beta \left(I_{Mg}/I_{Control} \right)_{2A^*} \right) / \left(I_{Mg}/I_{Control} \right)_{2A^*/2C},$$

where $I_{CIQ}/I_{Control}$ is the ratio of current in the presence of CIQ to that in the absence of CIQ at NR1/NR2C receptors (2.7) under these recording conditions (Supplementary Fig. S3). Similar calculations have been made for NR1/NR2D (Supplementary Fig. S2 and S3)

Patch clamp recording from HEK 293 cells

HEK 293 cells were maintained in 5% humidified CO₂ at 37°C in DMEM (Dulbecco's Modified Eagle Medium; Invitrogen, Carlsbad, CA) supplemented with 10% fetal bovine serum, 10 units/ml penicillin, and 10 μg/ml streptomycin and were transiently transfected using the Fugene 6 transfection reagent with cDNAs encoding NMDA receptor subunits and GFP at a ratio (NR1:NR2:GFP) of 1:1:1 or 1:1:5 (2 μg total DNA) for 12-16 hrs³⁶. Current responses from voltage-clamp recordings of HEK cells ($V_{HOLD} = -60$ mV) and outside-out patches ($V_{HOLD} = -80$ mV) were filtered at 8 kHz (8 pole Bessel filter, -3 dB) and digitized at 20-40 kHz. The extracellular solution consisted of (in mM) 150 NaCl, 10 HEPES, 0.5 CaCl₂, 3 KCl, 0.01 EDTA, and 30 D-mannitol (pH 7.4). The internal solution consisted of (in mM) 110 D-gluconate, 110 CsOH, 30 CsCl₂, 5 HEPES, 4 NaCl, 0.5 CaCl₂, 2 MgCl₂, 5 BAPTA, 2 NaATP, 0.3 NaGTP (pH adjusted to 7.35 with CsOH). For whole-cell patch recordings, rapid solution exchange was achieved with a two-barrel theta glass pipette controlled by a piezoelectric translator. Open tip junction currents typically had 10-90% rise times of 1 ms or less; solution exchange around a whole cell was determined by changing the concentration of extracellular potassium, which altered the leak current with a 10-90% rise time of 5 ms³⁷. Single channel recordings from outside-out patches were performed at pH 8.0 using steady state application of agonist. All recordings were performed at 23°C unless otherwise indicated.

Patch clamp recording from neurons in thin slices

Rats (Sprague-Dawley, age P10 to P17) were anaesthetized using isoflurane, decapitated, and the brain was hemisected and glued to the stage of a vibrating microtome (Leica VT1000S). Sagittal brain slices were cut in cold artificial cerebrospinal fluid (ACSF) composed of (in mM) 130 NaCl, 24 NaHCO₃, 10 glucose, 3 KCl, 3 MgSO₄, 1.25 NaH₂PO₄, and 1 CaCl₂ and incubated at room temperature in the same solution for at least one hour before use. Slices containing the subthalamic nucleus or hippocampus were placed in the recording chamber of an upright microscope for whole cell voltage-clamp recordings. Slices were perfused with ACSF comprised of (in mM) 130 NaCl, 24 NaHCO₃, 10 glucose, 3 KCl, 1.5 MgSO₄, 1.5 CaCl₂, and 1.25 NaH₂PO₄ saturated with 95% O₂ / 5% CO₂ at pH 7.4 (23°C). Voltage-clamp recordings were performed at -60 mV, filtered at 5 kHz, and digitized at 20 kHz. Patch recording electrodes were filled with (in mM) 115 K-methylsulfate, 20 NaCl, 10 phosphocreatine, 5 HEPES, 2 Mg-ATP, 1.5 MgCl₂, 1 QX-314, 0.5 Na-GTP, and 0.1 EGTA at pH 7.5. Recording solutions contained 0.2 mM MgSO₄, 0.5 μM TTX, 10 μM bicuculline, and 5 μM nimodipine. Currents were evoked when NMDA (1-2 mM) and glycine (0.5-1 mM) were pressure-applied through a borosilicate capillary tube (3.5 MOhm) in brief pulses (4-12 psi; 3-100 ms) using a Picospritzer II (Parker Hannifin Corp). After 3-10 stable measurements were obtained in the presence of the control solution at 1 minute intervals, CIQ (20 μM, prepared in recording solution) or vehicle was bath applied for 10-15 min. Current responses evoked by pressure application of NMDA and glycine were compared to currents obtained during application of control ACSF. Following bath application of CIQ, the slice was washed with the control recording solution and NMDA and glycine continued to be pressure applied at a 1 minute interval to determine the degree of CIQ washout. The NMDA receptor competitive antagonist D,L-APV (200-400 μM) was subsequently bath applied during NMDA and glycine applications. The I_h current was recorded under current-clamp using the same intracellular solution by injecting 0.1 nA of current into the cell.

Synthesis and physicochemical properties of CIQ

CIQ, (3-chlorophenyl)(6,7-dimethoxy-1-((4-methoxyphenoxy)methyl)-3,4-dihydroisoquinolin-2(1H-yl)methanone (CIQ, C₂₆H₂₆ClNO₅; molecular weight of 467.94) was synthesized from commercially available starting materials (see Supplementary Methods and Fig. S1). CIQ is also commercially available and can be obtained from Life Chemicals (Orange, CT; catalogue # F0535-0139). Characterization and determination of purity was established by ¹H NMR, ¹³C NMR, high resolution mass spectrometry, and elemental combustion analysis. All experiments were conducted on the racemic mixture.

CIQ has a predicted Log P value of 4.95 from ChemDraw. The total polar surface area (i.e. van der Waals surface area of polar nitrogen and oxygen atoms) is 58.5 angstroms². The maximum solubility of CIQ was determined using a BMG Labtech Nephelostar nephelometer (Offenburg, Germany) according to manufacturer's instructions, and was 20 μM. CIQ did not form detectable micelles at 10 μM when dissolved in HEK 293 extracellular recording solution or in filtered H₂O, as assessed using a Malvern Instruments Zetasizer dynamic light scattering instrument (Worcestershire, UK). No detectable micelles or nanoparticles were observed during examination of evaporated solution with a Hitachi H-7500 transmission electron microscope (accelerated voltage 75kV; magnifications from 5-100 kx). CIQ was dissolved in 100% DMSO to make 200-2000x stock solutions that were then added directly to oocyte recording solutions to give a final solution containing a maximum of 0.05-0.5% DMSO. All recordings from mammalian cells used 1:1000-1:2000 dilution of 20 mM stock (0.05-0.1% DMSO). DMSO was not required for activity, as CIQ dissolved in 2-hydroxypropyl-beta-cyclodextrin solution (1% w/v) potentiated NR1/NR2D receptors responses in oocytes (144 ± 3% of control; n = 4). DMSO did not induce any

potentiation of NR1/NR2D responses in oocytes ($100 \pm 1.1\%$ of control; $n = 6$) or HEK cells (106 ± 7.7 , $n = 3$).

Molecular Biology

The following constructs encoding wild type NMDA receptor subunits were used: rat NR1-1a and all other rat NR1 splice variants (GenBank U11418, U08261; hereafter NR1), rat NR2A (D13211), rat NR2B (U11419), rat NR2C (M91563), and rat NR2D (L31611), modified as described¹⁵. Chimeric NR2 subunits containing portions of rat NR2A and NR2D were generated as previously described³⁸ using PCR strategies and verified by DNA sequencing. Detailed information about the NR2A-NR2D chimeric junctions is summarized in Supplementary Fig. S4. Amino acids are numbered according to full-length protein, including the signal peptide.

Data Analysis

Single channel recordings from outside-out patches were idealized using the SKM algorithm of QuB³⁹ (<http://www.qub.buffalo.edu>) for measurement of open probability, mean shut time, and opening frequency. Open probability was calculated as the total duration of time that all detected channels in the patch were open divided by the total recording time. Because we cannot be sure of the total number of channels, this measurement does not represent the probability that one channel will open, but rather is the product of the probability that one channel will open and the number of channels in the patch. In a subset of high quality patches with adequately low noise, segments in which no double openings were observed were idealized using time course fitting (SCAN; provided by Dr. David Colquhoun, University College London⁴⁰) for measurement of individual open and closed durations, mean open time, unitary current amplitudes, and chord conductances. Amplitude histograms were fitted by the sum of multiple Gaussian components, and open and closed duration distributions were fitted with the sum of 2-5 exponential functions using maximum likelihood methods⁴⁰.

The deactivation time courses of the current responses were fitted by two exponential components using

$$Response = Amplitude_{FAST} \exp(-time/\tau_{FAST}) + Amplitude_{SLOW} \exp(-time/\tau_{SLOW}),$$

where τ_{FAST} and τ_{SLOW} are the deactivation time constants. The concentration-effect relationships for agonists were fitted to the Hill equation where EC_{50} is the concentration of agonist that produces a half-maximally effective response and N is the Hill slope. The concentration-effect relationships for CIQ potentiation were fitted to

$$Percent \ Response = 100 / (1 + (EC_{50} / [concentration])^N),$$

where EC_{50} is the concentration of CIQ that produces a half-maximally effective potentiation and N is the Hill slope.

Statistical Analysis

Student's paired t -test (two tailed) or analysis of variance (Dunnett's, Tukey's post hoc test) was used for statistical comparisons, as appropriate ($p < 0.05$ was considered significant). All data are expressed as mean \pm s.e.m. Although concentration-response EC_{50} data are given as mean \pm s.e.m., statistical tests were performed on the $\log(EC_{50})$, because EC_{50} shows a lognormal distribution^{41,42}.

Supplementary Material

Refer to Web version on PubMed Central for supplementary material.

Acknowledgments

The authors thank Tim Acker and Kurt Pennell for assistance with physicochemical measurements, and Rugina Ali, Mark Farrant, Trine Kvist, Chris McBain, Maiken Hedegaard, Ken Pelkey, and Massimiliano Renzi for sharing unpublished data. This work was supported by the NIH-NINDS (NS036654, NS065371 SFT), the Lundbeck Foundation (KBH), the Villum Kann Rasmussen Foundation (KBH), the Michael J Fox Foundation (SFT), the Emory University Research Committee (SFT), the Georgia Tech/Emory Center for Engineering of Living Tissue and the Atlanta Clinical and Translational Science Institute (SFT), a Research Grant from Pfizer, Inc. (SFT), NIH-NIGMS training grant GM008602 (KKO), NIH-NIDA training grant DA01504006 (KMV), NIH-NIEHS training grant ES012870 (KMV), the Emory Chemistry Biology Discovery Center, and the Robert P. Apkarian Integrated Electron Microscopy Emory University Core.

References

1. Erreger K, Chen PE, Wyllie DJ, Traynelis SF. Glutamate receptor gating. *Crit. Rev. Neurobiol.* 2004; 16:187–224. [PubMed: 15701057]
2. Coyle JT, Tsai G, Goff D. Converging evidence of NMDA receptor hypofunction in the pathophysiology of schizophrenia. *Ann. N. Y. Acad. Sci.* 2003; 1003:318–327. [PubMed: 14684455]
3. Morris BJ, Cochran SM, Pratt JA. PCP: from pharmacology to modelling schizophrenia. *Curr. Opin. Pharmacol.* 2005; 5:101–106. [PubMed: 15661633]
4. Wang CX, Shuaib A. NMDA/NR2B selective antagonists in the treatment of ischemic brain injury. *Curr. Drug. Targets. CNS Neurol. Disord.* 2005; 4:143–151. [PubMed: 15857299]
5. Preskorn S, et al. An innovative design to establish proof of concept of the antidepressant effects of the NR2B subunit selective N-methyl-D-aspartate antagonist, CP-101,606, in patients with treatment-refractory major depressive disorder. *J. Clin. Psychopharmacol.* 2008; 28:631–637. [PubMed: 19011431]
6. Kalia L, Kalia S, Salter M. NMDA receptors in clinical neurology: excitatory times ahead. *Lancet Neurol.* 2008; 7:742–755. [PubMed: 18635022]
7. Hallett P, Standaert DG. Rationale for and use of NMDA receptor antagonists in Parkinson's disease. *Pharmacol. Ther.* 2004; 102
8. Stip E, Chouinard S, Boulay L. On the trail of a cognitive enhancer for the treatment of schizophrenia. *Prog. Neuropsychopharmacol. Biol. Psychiatry.* 2005; 29:219–232. [PubMed: 15694228]
9. Tamminga C. The neurobiology of cognition in schizophrenia. *J. Clin. Psychiatry.* 2006; 67:e11. [PubMed: 17081078]
10. Lisman JE, et al. Circuit-based framework for understanding neurotransmitter and risk gene interactions in schizophrenia. *Trends Neurosci.* 2008; 31:234–242. [PubMed: 18395805]
11. Williams K. Ifenprodil discriminates subtypes of the N-methyl-D-aspartate receptor: selectivity and mechanisms at recombinant heteromeric receptors. *Mol. Pharmacol.* 1993; 44:851–859. [PubMed: 7901753]
12. Fischer G, et al. Ro 25-6981, a highly potent and selective blocker of N-methyl-D-aspartate receptors containing the NR2B subunit. *J. Pharmacol. Exp. Ther.* 1997; 283
13. Avenet P, et al. Antagonist properties of eliprodil and other NMDA receptor antagonists at NR1A/NR2A and NR1A/NR2B receptors expressed in *Xenopus* oocytes. *Neurosci. Lett.* 1997; 223:133–136. [PubMed: 9089691]
14. Akazawa C, Shigemoto R, Bessho Y, Nakanishi S, Mizuno N. Differential expression of five N-methyl-D-aspartate receptor subunit mRNAs in the cerebellum of developing and adult rats. *J. Comp. Neurol.* 1994; 347:150–160. [PubMed: 7798379]
15. Monyer H, Burnashev N, Laurie DJ, Sakmann B, Seeburg PH. Developmental and regional expression in the rat brain and functional properties of four NMDA receptors. *Neuron.* 1994; 12:529–540. [PubMed: 7512349]

16. Watanabe M, Mishina M, Inoue Y. Distinct distributions of five NMDA receptor channel subunit mRNAs in the brainstem. *J. Comp. Neurol.* 1994; 343:520–531. [PubMed: 7518475]
17. Karadottir R, Cavalier P, Bergersen L, Attwell D. NMDA receptors are expressed in oligodendrocytes and activated in ischaemia. *Nature.* 2005; 438:1162–1166. [PubMed: 16372011]
18. Salter M, Fern R. NMDA receptors are expressed in developing oligodendrocyte processes and mediate injury. *Nature.* 2005; 438:1167–1171. [PubMed: 16372012]
19. Karavanova I, Vasudevan K, Cheng J, Buonanno A. Novel regional and developmental NMDA receptor expression patterns uncovered in NR2C subunit- β -galactosidase knock-in mice. *Mol. Cell. Neurosci.* 2007; 34:468–480. [PubMed: 17276696]
20. Standaert DG, Testa CM, Young A, Penney JB Jr. Organization of N-methyl-D-aspartate glutamate receptor gene expression in the basal ganglia of the rat. *J. Comp. Neurol.* 1994; 343:1–16. [PubMed: 8027428]
21. Wenzel A, Villa M, Mohler H, Benke D. Developmental and regional expression of NMDA receptor subtypes containing the NR2D subunit in rat brain. *J. Neurochem.* 1996; 66:1240–1248. [PubMed: 8769890]
22. Standaert DG, Landwehrmeyer BG, Kerner JA, Penney JB, Young AB. Expression of NMDAR2D glutamate receptor subunit mRNA in neurochemically identified interneurons in the rat neostriatum, neocortex and hippocampus. *Brain Res. Mol. Brain Res.* 1996; 42:89–102. [PubMed: 8915584]
23. Counihan T, et al. Expression of N-methyl-D-aspartate receptor subunit mRNA in the human brain: mesencephalic dopaminergic neurons. *J. Comp. Neurol.* 1998; 390:91–101. [PubMed: 9456178]
24. Jones S, Gibb AJ. Functional NR2B- and NR2D-containing NMDA receptor channels in rat substantia nigra dopaminergic neurones. *J. Physiol.* 2005; 569:209–221. [PubMed: 16141268]
25. Brothwell SLC, et al. NR2B- and NR2D-containing synaptic NMDA receptors in developing rat substantia nigra pars compacta dopaminergic neurones. *J. Physiol.* 2008; 586:739–750. [PubMed: 18033813]
26. Rudolf GD, et al. Expression of N-methyl-D-aspartate glutamate receptor subunits in the prefrontal cortex of the rat. *Neuroscience.* 1996; 73:417–427. [PubMed: 8783259]
27. Cauli B, et al. Classification of fusiform neocortical interneurons based on unsupervised clustering. *Proc. Natl. Acad. Sci. U. S. A.* 2000; 97:6144–6149. [PubMed: 10823957]
28. Porter J, et al. Properties of bipolar VIPergic interneurons and their excitation by pyramidal neurons in the rat neocortex. *Eur. J. Neurosci.* 1998; 10:3617–3628. [PubMed: 9875341]
29. Hatton CJ, Paoletti P. Modulation of triheteromeric NMDA receptors by N-terminal domain ligands. *Neuron.* 2005; 46:261–274. [PubMed: 15848804]
30. Traynelis SF, Hartley M, Heinemann SF. Control of proton sensitivity of the NMDA receptor by RNA splicing and polyamines. *Science.* 1995; 268:873–876. [PubMed: 7754371]
31. Wyllie DJA, Behe P, Colquhoun D. Single-channel activations and concentration jumps: comparison of recombinant NR1a/NR2A and NR1a/NR2D NMDA receptors. *J. Physiol.* 1998; 510:1–18. [PubMed: 9625862]
32. Stern P, Behe P, Schoepfer R, Colquhoun D. Single-channel conductances of NMDA receptors expressed from cloned cDNAs: comparison with native receptors. *Proc. R. Soc. Lond. B. Biol. Sci.* 1992; 250:271–277.
33. Yuan H, Hansen KB, Vance KM, Ogden KK, Traynelis SF. Control of NMDA receptor function by the NR2 subunit amino-terminal domain. *J. Neurosci.* 2009; 29:12045–12058. [PubMed: 19793963]
34. Sobolevsky AI, Rosconi MP, Gouaux E. X-ray structure, symmetry and mechanism of an AMPA-subtype glutamate receptor. *Nature.* 2009; 462:745–756. [PubMed: 19946266]
35. Traynelis SF, Burgess MF, Zheng F, Lyuboslavsky P, Powers JL. Control of voltage-independent zinc inhibition of NMDA receptors by the NR1 subunit. *J. Neurosci.* 1998; 18:6163–6175. [PubMed: 9698310]
36. Dravid SM, Prakash A, Traynelis SF. Activation of recombinant NR1/NR2C NMDA receptors. *J. Physiol.* 2008; 586:4425–4439. [PubMed: 18635641]

37. Erreger K, Traynelis SF. Allosteric interaction between zinc and glutamate binding domains on NR2A causes desensitization of NMDA receptors. *J. Physiol.* 2005; 569:381–393. [PubMed: 16166158]
38. Chen PE, et al. Modulation of glycine potency in rat recombinant NMDA receptors containing chimeric NR2A/2D subunits expressed in *Xenopus laevis* oocytes. *J. Physiol.* 2008; 586:227–245. [PubMed: 17962328]
39. Qin F. Restoration of Single-Channel Currents Using the Segmental k-Means Method Based on Hidden Markov Modeling. *Biophys. J.* 2004; 86:1488–1501. [PubMed: 14990476]
40. Colquhoun, D.; Sigworth, FJ. Single-Channel Recording. Sakmann, B.; Neher, E., editors. Plenum Press; 1995. p. 483-587. Ch. 19
41. Gaddum JH. Lognormal Distributions. *Nature.* 1945; 156:463–466.
42. Christopoulos A. Assessing the distribution of parameters in models of ligand-receptor interaction: to log or not to log. *Trends Pharmacol. Sci.* 1998; 19:351–357. [PubMed: 9786022]

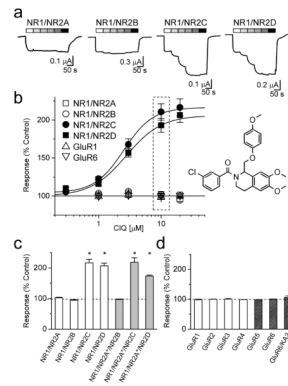


Figure 1.

CIQ selectively potentiates NR2C and NR2D subunits.

- a. Two-electrode voltage-clamp recordings of recombinant NMDA receptors expressed in *Xenopus* oocytes and activated by 100 μ M glutamate plus 30 μ M glycine in the absence and presence of increasing concentrations of CIQ (1 – 100 μ M).
- b. Concentration-response curves show the subunit-selectivity of CIQ ($n = 18-21$ oocytes per receptor). The response to 100 μ M glutamate and 30 μ M glycine in the absence of CIQ is normalized to 100%. The structure of CIQ is shown at the right. The dashed box highlights the concentration (10 μ M) of CIQ that produces potentiation of responses from NR1/NR2C (●) and NR1/NR2D (■) without affecting responses from NR1/NR2A (□), NR1/NR2B (○), AMPA (GluR1, Δ), and kainate (GluR6, ∇) receptors. c. The responses of wild type diheteromeric NMDA receptors to 10 μ M CIQ plus 100 μ M glutamate and 30 μ M glycine are shown as a percentage of the response in the absence of CIQ (100%). The responses of NR1/NR2C and NR1/NR2D in the presence of CIQ were significantly different than in control (* $p < 0.05$; paired t-test; $n = 6 - 14$). The responses of triheteromeric NMDA receptors containing NR2A(N614K,T690I) (hereafter NR2A*) to 10 μ M CIQ in the presence of 10 mM glutamate, 100 μ M glycine, and 1 mM Mg^{2+} are shown as a percentage of the response in the absence of CIQ (100%). While triheteromeric receptors composed of NR1/NR2A*/NR2B were not potentiated by CIQ, NR1/NR2A*/NR2C, and NR1/NR2A*/NR2D triheteromeric receptors were significantly potentiated by CIQ (* $p < 0.05$; paired t-test; $n = 8 - 18$).
- d. The responses of GluR1, GluR2, GluR3, GluR4, GluR5, and GluR6 receptors to 100 μ M glutamate in the presence of 10 μ M CIQ are not significantly different than control ($n = 4 - 10$); oocytes expressing GluR5 and GluR6 were exposed to 10 μ M concanavalin-A for 10 minutes prior to recording. Responses of GluR6/KA2 receptors were evoked by 100 μ M AMPA. For all panels, values are mean \pm s.e.m.

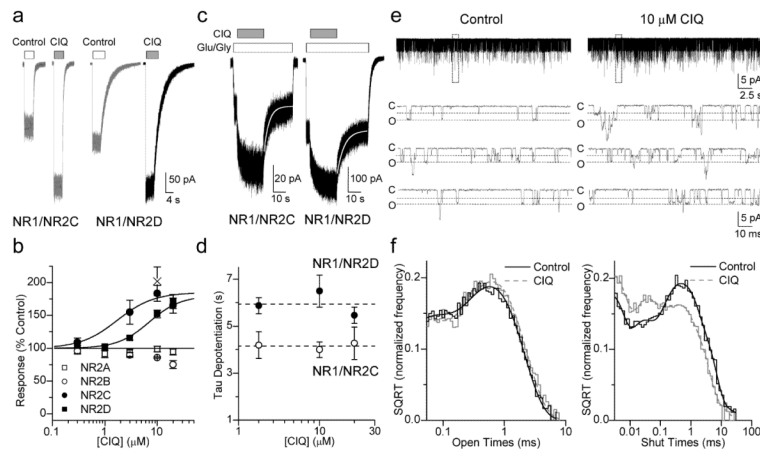


Figure 2.

CIQ selectively potentiates NR1/NR2C and NR1/NR2D receptors in HEK 293 cells.

a. Representative whole-cell voltage-clamp recordings of NR1/NR2C and NR1/NR2D at 23°C. CIQ (10 μ M in 100 μ M glutamate and 30 μ M glycine) evokes 180% responses from both NR1/NR2C and NR1/NR2D compared to control (100 μ M glutamate and 30 μ M glycine).

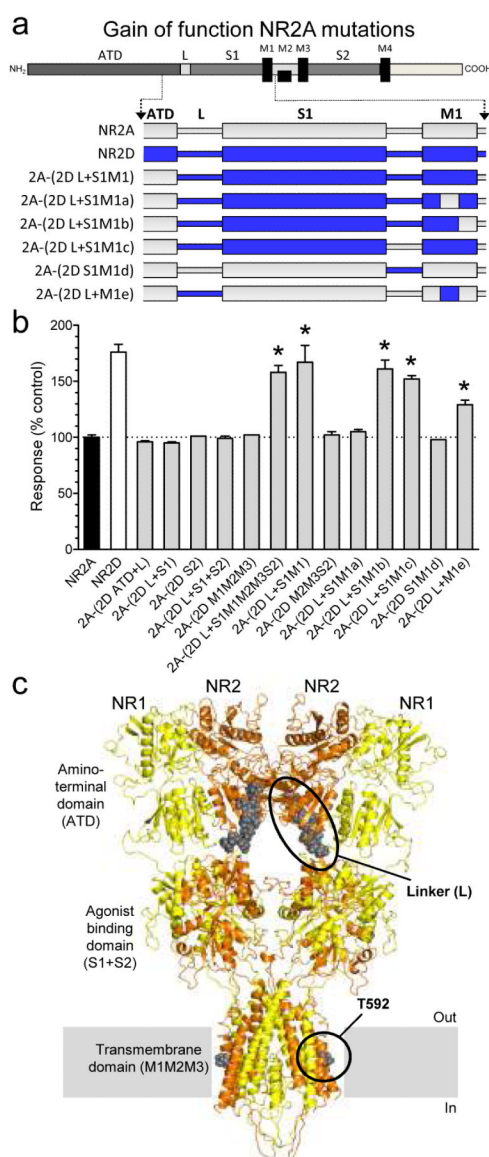
b. The concentration-effect relationships demonstrate CIQ selectively potentiates NR1/NR2C (\bullet , $EC_{50} = 1.7 \mu$ M; $n = 5-11$) and NR1/NR2D (\blacksquare , $EC_{50} = 4.1 \mu$ M; $n = 4-17$) to 180% in mammalian cells, but has no effect on NR1/NR2A (\square , $n = 4-15$). CIQ causes a modest (25%) reduction in the NR1/NR2B response at 20 μ M (\circ , $n = 5$). CIQ (10 μ M) potentiated the response of NR1/NR2D to NMDA at 33°C by $200 \pm 20\%$ ($n = 5$, \times on plot). Values are mean \pm s.e.m.

c. Current responses of NR1/NR2C (\circ) and NR1/NR2D (\bullet) receptors to 100 μ M glutamate and 30 μ M glycine (white bar) and concurrent application of 10 μ M CIQ (gray bar) show that the de-potentialization time course is described by a single exponential function (white line; ³³).

d. The de-potentialization time course is independent of CIQ concentration for NR1/NR2C ($n = 3$) and NR1/NR2D receptors ($n = 6$). Values are mean \pm s.e.m.

e. Unitary currents from a representative outside-out patch containing NR1/NR2D receptors activated by 1 mM glutamate and 50 μ M glycine in the absence or presence of 10 μ M CIQ. The boxed region is expanded below; *c* denotes the closed and *o* the open level.

f. Composite distributions of the contiguous open period durations from 6 patches can be fitted by two exponential components with time constants of 0.044 ms and 0.57 ms for control and 0.036 ms and 0.63 ms for CIQ (see also Table 1). The composite closed duration histogram constructed from recordings in the same 6 patches can be fitted by the sum of 6 exponential components, with time constants (area in parentheses) of 0.022 (29), 0.19 (14), 1.7 (12), 5.5 (27), 19 (17) and 94 (0.4) ms in the absence and 0.026 (37), 0.23 (18), 0.73 (12), 3.4 (18), 12 (15) and 39 (0.75) ms in the presence of 10 μ M CIQ.

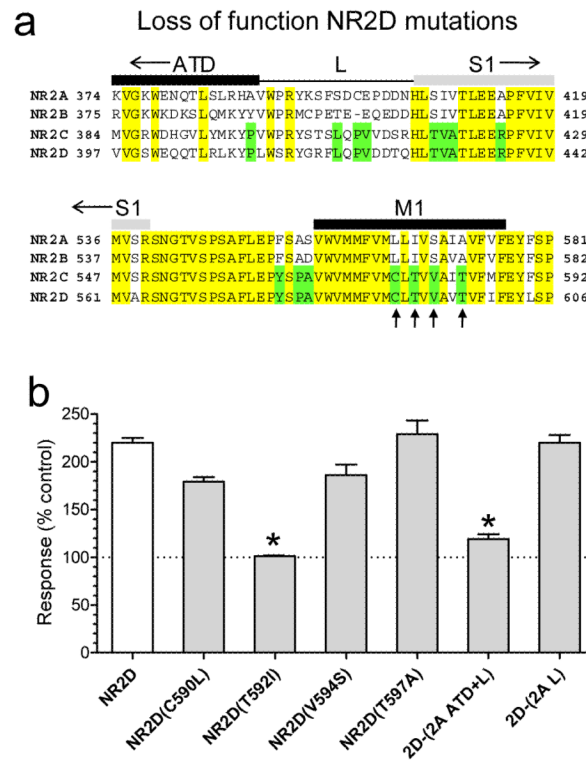
**Figure 3.****Structural determinants for transferring CIQ sensitivity to NR2A**

a. Schematic representation of the NR2 subunit polypeptide illustrates regions comprising the amino-terminal domain (ATD), the agonist binding domain (two segments of the polypeptide chain called S1 and S2), a membrane-associated domain that forms the ion channel pore and contains three membrane-spanning helices (M1, M3, M4) with a re-entrant loop (M2), and an intracellular C-terminal domain. Schematic representations of chimeras between the NR2D ATD-M1 region and the corresponding region in NR2A are shown (see Supplementary Table S4 for chimeric junctions).

b. The response to 10 μ M CIQ plus 100 μ M glutamate and 30 μ M glycine is shown as a percentage of the response in the absence of CIQ. CIQ sensitivity is observed ($p < 0.05$ compared to wild type NR2A; one-way ANOVA with a Dunnett's post test) for chimeras 2A-(2D L+S1M1M2M3S2), 2A-(2D L+S1M1), 2A-(2D L+S1M1b), 2A-(2D L+S1M1c), and 2A-(2D L+M1e), suggesting transfer of CIQ sensitivity to NR2A requires residues

590-594 from NR2D and the NR2D linker region (L) between the ATD and the S1 region. Results are from 4-23 oocytes per receptor tested. Values are mean \pm s.e.m.

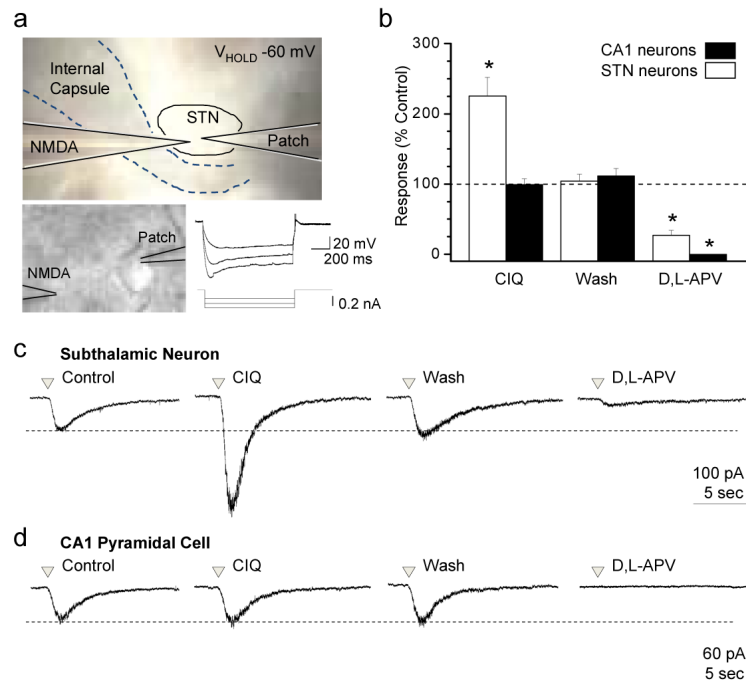
c. Model of an NR1/NR2 heterodimer of the tetrameric NMDA receptor based on the GluR2 structure³⁴ is shown. M4 and the C-terminal domain are omitted for clarity. The NR1 and NR2 subunits are shown in yellow and brown, respectively. The regions that together can transfer CIQ sensitivity from NR2D to NR2A (T592 and the ATD-S1 linker) are shown as grey spheres and highlighted in black circles.

**Figure 4.**

Structural determinants of CIQ action in NR2D

a. Alignment of amino acid sequences for the ATD-S1 linker and M1 regions of NR2A-D. Fully conserved residues are shown in yellow, and residues conserved only in NR2C and NR2D are shown in green. Arrows mark residues that were converted in NR2D from the NR2C/D residue to the NR2A/B residue and *vice versa* by site-directed mutagenesis (Supplementary Table S4).

b. Four M1 residues in NR2D that are conserved between NR2C/D but not NR2A/B were mutated to the corresponding residue in NR2A/B. Responses of the mutant receptor NR1/NR2D(T592I) were no longer potentiated by CIQ. Chimeric NR2D receptors with the ATD +L showed a reduced level of potentiation. Results are from 6-10 oocytes per receptor tested. *, $p < 0.05$ compared to NR1/NR2D, one-way ANOVA with a Tukey's post hoc test). Values are mean \pm s.e.m.

**Figure 5.**

CIQ potentiates native NR2D-containing NMDA receptors in subthalamic neurons

a. Photomicrograph of the experimental setup for whole cell voltage-clamp recording from subthalamic (STN) neurons. A pressurized (4-12 psi; 3-100 ms application) micropipette (3.5 MOhm) was used to apply glycine (0.5-1 mM) and NMDA (1-2 mM) to the subthalamic neuron, which was held at -60 mV . *Lower right*, neurons demonstrated characteristic I_h current, evoked by injecting 0.1 nA hyperpolarizing current into the cell.

b. CIQ (20 μM) potentiated STN neurons to $230 \pm 29\%$ ($n = 6$; white bars) compared to the control response. Potentiation by CIQ was reversible, with NMDA-activated responses after recovery being $102 \pm 11\%$ of control amplitude. NMDA-activated responses could be inhibited by the NMDA receptor competitive antagonist D,L-APV (200-400 μM ; $27 \pm 7\%$ residual current compared to control). CIQ did not potentiate the current response to pressure-applied NMDA in hippocampal CA1 pyramidal neurons ($n = 5$; black bars). Data are mean \pm s.e.m. * $p < 0.01$; one-way ANOVA with repeated measures and Tukey's *post hoc* test.

c. Representative whole cell-voltage clamp recordings of the current response to pressure-applied NMDA/glycine in a subthalamic neuron shows that CIQ potentiation was reversible, and that NMDA-evoked currents were inhibited by D,L-APV.

d. Representative whole cell voltage-clamp recording from a hippocampal CA1 pyramidal neuron in response to pressure-applied NMDA and glycine demonstrates that CIQ potentiation is selective for GluN2C/D-containing receptors over GluN2A/B-containing receptors.

Table 1

CIQ has minimal effects on glutamate or glycine EC₅₀

EC₅₀ values were obtained as described in the *Methods*; * indicates p<0.05 compared to control for log(EC₅₀) values (t-test).

	Control		+ 20 μM CIQ	
	EC ₅₀ (μM)	Slope n	EC ₅₀ (μM)	Slope n
NRI/NR2C				
Glutamate	0.74 ± 0.06	1.5 6	0.62 ± 0.04	1.5 8
Glycine	0.24 ± 0.03	1.5 8	0.23 ± 0.02	1.6 6
NRI/NR2D				
Glutamate	0.30 ± 0.03	1.5 6	0.24 ± 0.02	1.6 6
Glycine	0.15 ± 0.01	1.5 5	0.12 ± 0.01*	1.4 6

Table 2

CIQ has minimal effects on NMDA receptor deactivation

The time course describing deactivation following removal of glutamate was fitted with two exponential components (see *Methods*), as previously described.^{31,8} The average time constants are shown, and the amplitude for the slow component is given in parentheses; Glycine (30 μ M) was present in all solutions.

	Control		+ 10 μ M CIQ		n
	τ_{FAST} (ms)	τ_{SLOW} (%)	τ_{FAST} (ms)	τ_{SLOW} (%)	
NRI/NR2A	40 \pm 4	560 \pm 140 (15)	45 \pm 4	640 \pm 160 (5)	9
NRI/NR2B	310 \pm 30	1100 \pm 190 (40)	320 \pm 30	1100 \pm 120 (40)	5
NRI/NR2C	110 \pm 30	310 \pm 35 (50)	200 \pm 30 *	530 \pm 60 *	7
NRI/NR2D	2100 \pm 150	5700 \pm 510 (53)	2000 \pm 270	5800 \pm 600 (60)	13

* indicates $p < 0.05$ (paired t-test).

Table 3
NR1/NR2D channel properties in the presence of CIQ

NR1/NR2D channel currents were recorded as described in the *Methods*. For open duration time constants τ_1 and τ_2 and chord conductances γ_1 and γ_2 , the relative corresponding areas are given in parentheses. All values are mean \pm s.e.m.; P_{OPEN} is the probability of at least one receptor being open within patches, which all contained two or more channels. $n = 11$ for P_{OPEN} , opening frequency and mean shut time and $n = 6$ for mean open time, τ_1 , τ_2 , amplitude-1, amplitude-2, γ_1 , and γ_2 .

	Control	+ 10 μM CIQ
P_{OPEN}	0.15 ± 0.03	$0.29 \pm 0.07^*$
P_{OPEN} (%)	100	$190 \pm 25^*$
Opening Frequency (Hz)	208 ± 40	$303 \pm 57^*$
Opening Frequency (% control)	100	$148 \pm 17^*$
Mean shut time (ms)	6.8 ± 1.2	$5.4 \pm 1.3^*$
Mean open time (ms)	0.57 ± 0.03	0.64 ± 0.05
Open τ_1 , ms (%)	0.044 ± 0.005 (29)	0.036 ± 0.003 (25)
Open τ_2 , ms (%)	0.57 ± 0.03 (71)	0.63 ± 0.06 (75)
Amplitude-1 (pA)	2.6 ± 0.09	$2.5 \pm 0.1^*$
Amplitude-2 (pA)	4.4 ± 0.09	$4.3 \pm 0.1^*$
γ_1 , pS (%)	33 (23)	31^* (29)
γ_2 , pS (%)	56 (77)	54^* (71)

* indicates $p < 0.05$ vs. control (paired, two-tailed t test).